

maximum. The amplitude α increases toward the solar activity minimum. It is shown that the pattern of variation in the inclination of the zones lying toward the equator as a function of the phase of solar activity cannot account for these peculiar features.

Analogy between the Structure of the Solar System and the Structure of the Galaxy and Other Spirals, M. S. Eïgenzon, pp 106-108

In a previous paper we were concerned with the principle of 'vertical' cosmological similarity. According to this principle, cosmic structures of different orders of magnitude exhibit certain well-known similarities. One of the examples where this principle applies is the similarity between the structure of globular stellar clusters and centrally symmetric clusters of galaxies. These structures in their turn are similar, in the radial distribution of the volume density of a number of structural elements, to an isothermal gaseous sphere. Another important example is the similarity between the structural dynamic properties of the solar system and spirals in general, and our galaxy in particular. The physical basis of this similarity is frequently found in the fact that the mechanism responsible for the formation of the given structure is, generally speaking, apparently preserved at neighboring structural "stages."

Derivation of the Period and Direction of Rotation of Venus from Radio Observations, A. D. Kuz'min and A. E. Salomonovich, pp 116-118

A procedure is described for identifying a periodic component in the variation of Venus' mean brightness temperature. A method is proposed for determining the direction of rotation from the variation of the apparent rotational velocity.

Thermal Conductivity of Lunar Material from Precise Measurements of Lunar Radio Emission, V. D. Krouikov and V. S. Troitskii, pp 119-120

Precise measurements of lunar radio emission yield a value for $\gamma = (K\rho C)^{-1/2}$, averaged over the lunar disk, of 350 ± 75 . With our previous value of $\rho \approx 0.5$ g/cm³ for the density of lunar material, this gives a coefficient of thermal conductivity of $K = (1 \pm 0.5) \cdot 10^{-4}$ cal/cm sec deg, a value almost 50 times the generally accepted value corresponding to dust in a vacuum. Contrary to current ideas, the upper layer of lunar material does not consist of dust, but is solid porous material perhaps somewhat pulverized.

SOVIET PHYSICS—SOLID STATE (Fizika Tverdogo Tela) Published by American Institute of Physics, New York

Volume 3, Number 11, May 1962

Kinetics of Photoconductivity in Neutron Irradiated *p*-Type Silicon, A. F. Plotnikov, V. S. Vavilov, and L. S. Smirnov, pp 2363-2367

The paper presents data relating to the concentration of defects introduced into *p*-type silicon by a fast neutron flux. The hole capture cross sections of these defects are evaluated; this permits one to arrive at certain conclusions concerning the charge of the defects.

Investigation of the kinetics of impurity photoconductivity has proved to be an effective method for determining various parameters of the impurity centers or defects which are present in the semiconductor crystals under observation. By studying the kinetics of the photoconductivity associated with excitation of current carriers to levels located in the forbidden gap, one can determine the concentration of centers in the crystal, their carrier-capture cross section, the degree of filling these impurity levels, and other characteristics of the centers.

The purpose of this paper is to examine the kinetics of photoconductivity in *p*-type silicon monocrystals which had been subjected to irradiation by a fast neutrons flux.

Photomagnetic Effect in *p*-Type InSb at Room Temperature, V. F. Zolotarev and D. N. Nasledov, pp 2400-2404

Studies have been made of the photomagnetic effect (PME) in *p* type InSb at room temperature over a range of impurity concentrations from $1.2 \cdot 10^{16}$ to $1.3 \cdot 10^{17}$ cm⁻³ and in magnetic fields from 600 to 16 000 oe. It appears that the mobility of electrons

determined from the photomagnetic effect on the basis of the phenomenological theory of PME differs from that determined from the Hall effect and conductivity. This difference depends on the concentration of acceptors in InSb. There is a dependence of the ambipolar diffusion length on magnetic field strength, but it appears that this dependence only partly determines the variation in short-circuited photomagnetic current with change in magnetic field strength. On the basis of these investigations it is concluded that there is closer agreement between experiment and PME theory based on the solution of the kinetic equation for the current through the specimen than there is between experiment and the phenomenological theory of PME. It is found that the hole mobility in *p*-type InSb at room temperature and at small impurity concentrations is not less than 1700 cm²/v sec, which agrees more closely with the theoretically predicted value of 3600 cm²/v sec than does the value of 750 cm²/v sec given in the literature.

It is observed that on illuminating a thin specimen first on a mechanically polished surface and then on an electrolytically polished surface, the photomagnetic effect changes sign. This change is due to absorption of light within the specimen.

Long-Time Changes of the Contact Potential of Certain Metals under the Action of Light, M. C. Kosman and S. M. Gorodetskii, pp 2429-2433

This paper contains a description of experimental investigations of the change in contact potential of aluminum, magnesium, and zinc after illumination. The results obtained agree with the model of Kingston and McWhorter, as improved by Abkevich, which is appreciable to surfaces of metals coated by oxide film. Within the framework of this model we explain the changes in shape of the relaxation curves for the change in the contact potential observed during absorption of water vapor.

Method of Green's Functions in the Theory of Adiabatic Approximation, S. V. Tyablikov, pp 2500-2509

The method of two time temperature-dependent Green's functions is used to study in the adiabatic approximation the problem of the interaction of a particle (or a system of particles) with a quantized field. In this way the results of the adiabatic theory of perturbations are extended to the case of temperatures different from zero.

Effects of γ Irradiation on the Spectral Distribution of Photosensitivity of CdS Monocrystals, T. Ya. Sera, V. V. Serdyuk, and I. M. Shevchenko, pp 2568-2569

Volume 3, Number 12, June 1962

Electrical Properties of Amorphous Films and Tellurium and the Effect of Additions on Their Crystallization, Yin Shih-tuan and A. R. Regel', pp 2627-2631

A study has been made of the temperature dependence of amorphous films of pure tellurium and of tellurium containing 0.5 at % iodine and 0.1 at % selenium. The effect of oxygen pressure on the crystallization of amorphous films has been investigated in the case of pure tellurium, and the thermal emf has also been measured. The hole concentration and the hole mobility have been calculated from electrical-conductivity and thermal emf data for amorphous films of pure tellurium. The hole concentration equals $\sim 10^{17}$ cm⁻³, and the mobility $\sim 10^{-2}$ cm²/v sec. Both quantities are almost independent of temperature, which is a new phenomenon in amorphous materials. The experimental results are explained qualitatively on the basis of the concept that amorphous tellurium films consist of a mixture of ring and chain molecules.

Thermoelectric Properties of Solid Solutions, Mg₂Si-Mg₂Sn, E. N. Nikitin, V. G. Bazanov, and V. I. Tarasov, pp 2648-2651

It was undertaken to make a material with favorable thermoelectric characteristics based on a solid solution of Mg₂Si-Mg₂Sn. The thermoelectric power, electrical conductivity, thermal conductivity, and their temperature dependences were investigated. The thermoelectric efficiency of the alloy Mg₂Si_{0.7}Sn_{0.3} doped with antimony was determined which on the average has $Z = 0.7 \cdot 10^{-3}$ per degree in the temperature interval 200-600°C. A study of the Hall effect showed that the dependence of the thermoelectric power on the concentration of current carriers differs from the theoretical formula of Pisarenko.

Change of Mechanical Properties of Germanium with Changing Concentration of Current Carriers, N. Ya. Gorid'ko, P. P. Kuz'menko, and N. N. Novikov, pp 2652-2656

In this work, the change in microhardness of a surface layer of germanium was studied as the concentration of free current carriers was varied. The concentration of current carriers was changed by varying the illumination of the germanium surface and by introducing minority carriers by injection from a point contact. On the basis of data available in the literature, a possible explanation is given for the mechanism of the change in toughness properties of germanium with change of the number of free carriers. An effect also detected was a change of the surface properties of germanium that had been exposed to light for a long time. This is probably caused by a regrouping of dislocations in the specimen during the time of illumination.

Volume 4, Number 1, July 1962

Effect of Low-Temperature Deformation on Subsequent Aging in Armco Iron, N. N. Davidenkov and V. D. Yaroshevich, pp. 5-8

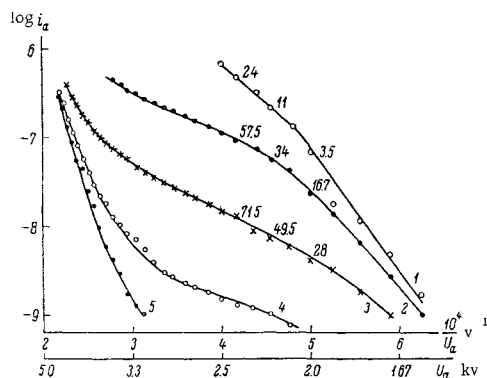


Fig. 1 Volt-ampere characteristics of a field current from CdS single crystals at different illuminations L at room temperature (unresolved white light, intensity changed by neutral filters): 1) L_0 ; 2) $10^{-1} L_0$; 3) $10^{-2} L_0$; 4) $10^{-3} L_0$; 5) without illumination. Numbers on curves are values of ΔV_k measured for a particular point on the curve.

We have studied the aging of armco iron specimens after deformation at temperatures of 20°, -78°, and -196°C. Diagrams for the deformation of aged specimens show that after deformation at -196°C aging is not accompanied by the appearance of a sharply defined yield point.

Apart from its practical importance, the study of the deformation aging of metals and alloys is of considerable interest of the development of ideas on the mechanism of plastic deformation. It is accepted that deformation aging and related effects are due to the redistribution of impurities in the volume of the metal. According to other papers, after plastic deformation the impurities interact with the free dislocations, diffuse toward them, and fasten onto them, forming characteristic "clouds" around them. After saturation of these "clouds," further aging proceeds by the precipitation of particles of carbides, nitrides, etc., which, in their turn, resist the motion of dislocations.

A characteristic feature of all investigations into deformation aging up to the present time is the fact that the connection between deformation and subsequent aging has been studied for the case where the preliminary deformation of the specimens was carried out at room temperature. The only work in which the aging was studied after preliminary deformation at temperatures below 0°C was reported in another paper. This paper mentions that preliminary deformation at -78°C leads to an increase in the rate of deformation aging. Aging was studied on iron produced by zone melting.

The aim of our investigation was to study effects of deformation aging (the appearance of a reproducible yield point, the shape of the deformation curve, etc.) after preliminary plastic deformation carried out at low temperatures.

Thermoelectromotive Force in Bismuth and Bismuth-Tellurium Alloys, D. V. Gitsu, G. A. Ivanov, and A. M. Popov, pp. 15-19

Results of thermo emf measurements on single crystals of bismuth and its alloys with tellurium are reported. It is shown that in pure bismuth the thermo emf has a large anisotropy. This

anisotropy $\alpha/\alpha_{\parallel}$ falls sharply with addition of tellurium and practically disappears in Bi-Te alloys containing more than 0.1 at % tellurium. The observed disappearance of the anisotropy is in accordance with theory.

It is to be noted that in anisotropic semiconductors greater anisotropy of the thermo emf is to be expected in the region of intrinsic conductivity than in the region of impurity conductivity where anisotropy is generally absent.

Nonlinearity of the Volt-Ampere Characteristics of Field Emission from CdS Single Crystals, I. L. Sokol'skaya and G. P. Shcherbakov, pp. 31-36

The volt-ampere characteristics of field emission from CdS single crystals, plotted over a fairly wide range of currents and voltages, are usually nonlinear. We have shown that the rapid increase in field emission in strong fields is connected with a parallel increase in the concentration of carriers. Both can be ascribed to the excitation of additional carriers by the strong internal field. We have shown that in the medium range of voltages the current is proportional to concentration. We have proved experimentally that the increase in current with voltage in weak fields is due to the heating of the electron gas in the emitter.

1) In weak fields and at low electron concentrations in the emitter, the increase in concentration on illumination is compensated by a reduction in the knee of the zones, as a result of which the current is little affected by the illumination.

2) With increase in the internal field in the emitter, there is heating of the electron gas and this compensation does not occur; the current therefore begins to depend on the illumination. Furthermore, for higher energy electrons the barrier penetrability is greater, so the current increases as the electron gas is heated.

3) Broadening of the distribution function reaches a limit at $\Delta V_k = 15-20$ v; therefore in medium fields the current is proportional to the concentration in the bulk of the emitter.

4) Starting with $\Delta V_k = 150-200$ v there is generation of carriers by the strong internal field, the concentration increasing exponentially with ΔV_k and the current increasing with $1/U$ much more rapidly than according to an exponential law.

A comparison with the results of other papers shows that in these studies volt-ampere curves were obtained only for regions of strong and medium fields and there were no sections with a shape characteristic of weak fields. It can be confirmed that the volt-ampere characteristics given in those papers are a special case of the family of curves in Fig. 1 of the present article.

Mechanism of the External Photoeffect from Massive Photocathodes under the Action of X Rays, M. A. Rumsh, V. N. Shchemelev, and Kh. Prois, pp. 49-51

The formula proposed earlier for determining the quantum yield of the external photoeffect of massive photocathodes, caused by x rays, is critically discussed in this article. In an improved formula the primary photoelectrons and the Auger electrons are separately taken into account. The spectrum intervals for which photoelectrons play the main role, and those in which Auger electrons are of decisive importance, are determined. The spectral dependence of the quantum yield is determined more precisely on the basis of the new formula and experimental data on the wavelength dependence of the average absorption coefficient for photoelectrons.

Plasmon Spectra in In and InSb, L. A. Balabanova, M. M. Bredov, and B. A. Kotov, pp. 60-62

Using the technique described in another paper, the spectra of the characteristic electron energy losses in thin films of In and InSb were measured. An attempt was made to interpret the spectra from the standpoint of the theory of plasma oscillations and the theory of interband transitions. We suggest the technique of studying characteristic losses in order to investigate electron energy spectra in solids.

Temperature Dependence of Carrier Lifetime in Indium Antimonide, D. N. Nasledov and Yu. S. Smetannikova, pp. 78-86

The temperature dependence of the lifetime and diffusion length of current carriers was investigated in p - and n -type samples of indium antimonide with impurity concentrations between 10^{13} - 10^{15} cm $^{-3}$. It was shown that, as a result of processes of capture of nonequilibrium current carriers by traps, the life times of electrons and holes differ sharply at low temperatures ($T < 140^\circ\text{K}$). A band model of the semiconductor with two recombination levels in the forbidden band is considered, which

qualitatively explains the behavior of the experimental curves in the investigated temperature region

Application of Retarded and Advanced Green's Functions in the Theory of Ferromagnetism, E N Yakovlev, pp 127-130

A method is presented for calculating the spontaneous magnetization of a ferromagnetic substance by means of retarded and advanced Green's functions. The perturbation theory used to uncouple the chain of equations for the Green's functions gives already in first order a value of the spontaneous magnetization close to that obtained by Dyson and by Oguchi

Life to Rupture of Metals Subjected to Torsion, I E Kurov and V A Stepanov, pp 135-142

It is shown that the life to rupture under torsion for aluminum, zinc, and copper is an exponential function of the stress and of the inverse absolute temperature. However, the rupture activation energy in the case of torsion appears to be less than the corresponding value for tension. It was also established that the absolute values of the life to rupture for the cases of torsion and tension under identical maximum normal stresses may differ by several orders of magnitude

Reversible Optico-Hydrodynamic Phenomena in a Nonideal Exciton Gas, S A Moskalenko, pp 199-204

A study was made of the collective properties of interacting excitons which form a neutral gas in semiconductors. Use was made of macroscopic theory of nonideal Bose gas and the phenomenological theory of superfluidity. Hydrodynamic phenomena in exciton gas were compared with the properties of liquid helium

Investigation of Work Hardening of Copper by a Nuclear Magnetic Resonance Method, V S Pavlovskaya and Yu S Stark, pp 205-207

Work hardening of copper was investigated by a nuclear magnetic resonance method using the Cu^{63} isotope absorption line. It was shown that all changes in the absorption line can be explained by first order quadrupole interactions. Electric field gradients were estimated at nuclear sites. From these data, the distortion of the unit cells of the crystal lattice was determined for different degrees of work hardening

Dependence of the Hall Coefficient in P-Germanium on Magnetic Field Strength, P I Baranskii and R M Vinetskii, pp 208-210

Volume 4, Number 2, August 1962

Absorption and Photoconductivity of Activated Amorphous Selenium Films, G A Andreeva, pp 391-393

Optical absorption and photoconductivity were measured for amorphous selenium films containing tellurium, bismuth selenide, and bismuth telluride impurities. Some hypotheses are put forward about the role of the contact layer between selenium and a metal. It is reported that doping with small amounts of bismuth selenide produced additional photosensitivity with a maximum in the $680 \text{ m}\mu$ region. This usually occurs as the result of heat treatment

Diffusion of Selenium and Mercury in Solid and Liquid Tellurium, Sh Movlanov and A A Kuliev, pp 394-396

The diffusion of selenium and mercury in solid and liquid tellurium has been studied. A jump in the value of the diffusion coefficients of selenium and mercury is observed at the transition of the tellurium from the solid to the liquid state

The diffusion of impurities in semiconductors has recently aroused great interest, since one of the methods of alloying and forming p - n junctions is by the diffusion of a suitable element into a semiconductor. The literature now contains copious data on the diffusion of impurities in silicon and germanium, but there are practically no data on the diffusion of impurities in tellurium apart from those in a single paper. Moreover, no work has been devoted to studying diffusion of various elements in semiconductors in the liquid state, although diffusion in melts plays an important part in purifying materials by crystallization methods and, in particular, by zone recrystallization

The present paper reports the results of a determination of the diffusion coefficients of selenium and mercury in solid polycrystalline and liquid tellurium, using the radioisotopes Se^{75} and Hg^{203}

Nernst-Ettingshausen Effects in Degenerate Indium Antimonide, O V Emel'yanenko, F P Kesamanly, and D N Nasledov, pp 397-398

Diffusion and Solubility of Silver in Bismuth Telluride, B I Boltaks and N A Fedorovich, pp 400-401

The present paper summarizes the results obtained in a study of diffusion and solubility of silver in Bi_2Te_3 ; silver acts as a donor and the silver-doped telluride is an efficient material for negative branches of thermocouples

Monocrystal line ingots were grown by Bridgman's method. Grown crystals were of p -type with a conductivity of $\approx 500 \text{ ohm}^{-1} \text{ cm}^{-1}$ and a thermoelectric power of $\approx 200 \text{ }\mu\text{V}/^\circ\text{C}$. Two groups of samples were prepared: Some were cut parallel to the cleavage planes and others at right angles to these planes. A radioactive tracer, Ag^{110} , was used and the technique of removal of successive sections was employed. Diffusion annealing was carried out in argon filled ampoules

The results obtained showed that diffusion of silver in Bi_2Te_3 was strongly anisotropic. The rate of diffusion parallel to the cleavage planes was 3-5 orders of magnitude (the actual value depended on the temperature range) greater than at right angles to the cleavage planes

Negative Photoconductivity in Germanium at the Temperature of Liquid Helium, V P Dobrego and S M Ryvkin, pp 402-403

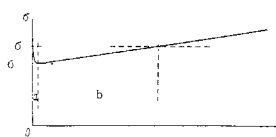


Fig 1 A typical lux-ampere characteristic

Negative photoconductivity (NPC) in germanium was found at liquid helium temperatures in n type samples which had a room-temperature resistivity of 0.2 – 0.4 ohm cm and in p type samples which had a room-temperature resistivity of 0.5 ohm cm . In n -type germanium with a resistivity of 1 ohm cm or more this effect was not observed. White light from an incandescent lamp was used. The dependence of the electrical conductivity on illuminance is given in Fig 1. At low intensities, illumination decreased the conductivity, i.e., a negative photoconductivity was observed. At higher intensities the more usual positive effect was superimposed on the NPC and swamped it

Volume 4, Number 4, October 1962

Gamma- and Photoelectric Properties of Cadmium Sulfide, P G Litovchenko and V I Ust'yanov, pp 773-774

The results are given of an experimental study of the gamma-conductivity and photoconductivity response spectra of cadmium sulfide crystals. A possible relationship between the two properties is established

Volume 4, Number 5, November 1962

Application of Functional Methods to the Theory of Solid Solutions, R A Suris, pp 850-857

Certain properties of solid solutions are investigated with functional methods similar to those used in the quantum theory of fields and in the many-body problem. The results obtained are valid for any system describable by the Ising model

The study of ordered binary alloys has been the object of a great number of theoretical articles (a detailed bibliography may be found in a reference noted). It is found that the problem admits an exact solution in the case of a two-dimensional lattice under the condition that the interaction is propagated only to the nearest neighbors. This solution cannot be generalized to the case of a three dimensional lattice. In this case one must resort to various approximate methods; however, the limits of applicability of such approximate methods is apparently still an unsettled question. There has appeared recently an interesting paper in which the method of quantum Green's functions was applied with success to the investigation of binary alloys

The present paper is devoted to the application of functional methods to the study of properties of solid solutions. Certain general operator expressions for the distribution function of atoms in a lattice will be obtained. These relations provide the possibility of obtaining approximate equations to which distribution functions are subjected, and they also clarify the

character of the approximations made. It will be shown that all quantities characterizing the lattice can be represented in the form of "functional integrals," which serve as convenient instruments for investigating the asymptotic behavior of the system for very large and very small dimensionless binding constants.

Theta-Function Expansion of the Dispersion Laws for Quasi-Particles in Crystals, A. B. Almazov, pp. 947-952

The paper describes a new method for investigating the dispersion laws for quasi-particles in crystals without any special assumptions regarding the form of the equations of motion. In the Fourier expansions of the dispersion laws the summation over the lattice sites is performed such that the expansions are converted into theta-function series or their derivatives. As an example, we studied the dispersion laws for holes in germanium and silicon. It is demonstrated that the theta expansions yield (at least qualitatively) all of the densities of states from the tight-binding approximation to the almost free quasi-particle approximation, inclusive, in a first approximation.

In this paper we propose a new method for investigating the expansions

$$E(\mathbf{k}) = E_0 + \sum_{\mathbf{s}} A(\mathbf{R}_{\mathbf{s}}) e^{i\mathbf{k}\mathbf{R}_{\mathbf{s}}} \quad (1)$$

Here $E(\mathbf{k})$ is the energy of a quasi-particle (an electron-hole exciton, a phonon, a spin wave); $\mathbf{R}_{\mathbf{s}}$ is the radius vector for the s th lattice site; the vector \mathbf{k} is specified on an enumerable set in the first Brillouin band; E_0 is a parameter which determines the energy origin. The subscript which numbers the band (the branch of the vibrations) is dropped, since all the subsequent analysis applies to the case where one band is treated. No special assumptions are made concerning the specific form of the equations of motion for the quasi-particles. Only the laws governing the transformations of expression (1) into each other for point transformations are assumed known. The proposed method differs from other methods and is based on transforming the Fourier expansions (1) into theta function expansions. Theta-function expansions can, as we shall demonstrate, be used to reconstruct the dispersion laws from individual experimental data on the basis of extrapolation and interpolation.

Several variants exist for determining theta-functions, which differ only slightly from one another. We shall make use of the following:

$$\begin{aligned} \vartheta_3(\chi) &= \vartheta_3(\chi; \alpha) = \sum_{n=-\infty}^{\infty} q^{n^2} e^{i2n\chi} \\ \vartheta_2(\chi) &= \vartheta_2(\chi; \alpha) = \sum_{n=-\infty}^{\infty} q^{(n-1/2)^2} e^{i(2n-1)\chi} \\ q &= e^{-\pi\alpha} \quad \vartheta_2(\chi + \pi/2) = -\vartheta_1(\chi) \\ \vartheta_3(\chi + \pi/2) &= \vartheta_4(\chi) \end{aligned}$$

The last two equations express the "quasi-periodicity" of the theta-functions: they can be transformed into each other (just as trigonometric functions) when the independent variable varies by a half period. The theta functions are written in the following abridged form for the zero values of the arguments:

$$\vartheta(r; \alpha) = \vartheta(r = 1, 2, 3, 4)$$

The modular angle is determined from the relationships

$$\frac{\vartheta_2^4}{\vartheta_3^4} = \sin^2 \theta \quad \frac{\vartheta_4^4}{\vartheta_3^4} = \cos^2 \theta$$

Properties of the Bloch and Wannier Functions, D. S. Bulyanitsa and Yu. E. Svetlov, pp. 981-985

It is demonstrated by functional analysis that the Bloch functions for everywhere nondegenerate zones are analytic functions of the components of the vector parameter \mathbf{k} . The results obtained are then used to study the Wannier functions. It is shown that in this case the Wannier functions decay asymptotically by an exponential law as the argument of the function increases. This result was obtained by Kohn for a one dimensional model. Some of the other properties of Wannier functions are examined.

by Various Methods, I. A. Akimov and E. K. Putseiko, pp. 1133-1137

It is known that in some cases the use of different methods to determine the internal photoeffect spectrum in the same semiconductor gives different results. For instance the photoconductivity spectra for cuprous oxide, selenium, silver bromide and silver chloride, diamond, mercury iodide, lead sulfide, indium antimonide and many others are displaced towards the long wave region compared with photo-emf spectra measured for the same semiconductors by the condenser method. Similar discrepancies arise in the case of photoconductivity spectra in the same semiconductors recorded with longitudinal and transverse illumination, respectively, and also in the case of zinc sulfide, cadmium sulfide, anthracene, etc. Noskov et al. have recently shown that the photomagnetic emf spectrum in cuprous oxide is displaced in the short-wave direction relative to the photoconductivity spectrum.

On the other hand, in a large group of organic and inorganic semiconductors, the photoconductivity spectrum frequently appears to be distorted relative to the absorption spectrum. In these cases we observe a decrease in the photoeffect yield in the region of strong absorption of the semiconductor and the appearance of a narrow photocurrent maximum in the descending branch of the optical absorption curve.

A number of authors have also shown that the location of the selective maximum and the photoconductivity spectrum in such semiconductors depend on the specimen thickness. Various hypotheses have been advanced in explanation of this complex behavior of the photoconductivity spectrum. Recently it has been widely assumed that the form of the photoconductivity spectrum is determined by the nature of the surface and bulk photocarrier recombination processes. In addition, it has been postulated that the appearance of a selective maximum at the absorption edge and the decrease in photocurrent in the region of strong absorption of the semiconductor is determined by an exciton mechanism of photocarrier creation. It follows from the foregoing that it is difficult to form definite conclusions concerning the nature of the photoresponse in the investigated semiconductors from an analysis of photoconductivity spectra.

In the present work we compared the spectral characteristics of the internal photoeffect determined by different methods in the same layers of a number of organic and inorganic semiconductors under the same conditions of illumination.

Spectral Distribution of the Internal Photoeffect in Photochemically Sensitive Semiconductors, I. A. Akimov, pp. 1138-1144

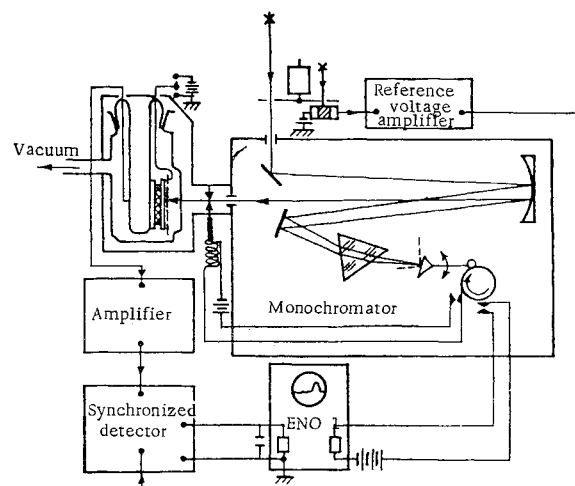


Fig. 1 Experimental arrangement for velocity measurement of the photo-emf spectrum in a condenser

A velocity method was used to investigate photoconductivity and photo emf spectra in dyed and undyed silver halides in microcrystalline powder form. Cyanine dyes were used and the measurements were carried out in the region from 350 to 1000 μ . The semiconductor was irradiated with energies of the order of 10^{-6} w/cm².

The change in the photoeffect in the region of the semiconductor absorption edge is explained by the formation of electron

trapping levels as a result of chemical decomposition of the silver halide. Experiments with dyed layers confirm the mechanism of energy transfer from the dye to the semiconductor and the importance of acceptor levels in the semiconductor in regard to optical sensitization.

Volume 4, Number 7, January 1963

Calculation of the Ionic and Atomic Components of the Bonds in Silicon Carbide Crystals, A. A. Tsertsvadze, Yu. V. Chkhartishvili, and Z. S. Kachlishvili, pp. 1278-1281

We have investigated the percentages of ionic and atomic binding in SiC crystals. We have considered a system of two electrons responsible for the bond between the nearest Si and C atoms. We have sought the wave function of this system in the form of a linear combination of functions corresponding to one atomic and two ionic states. The coefficients of these functions are found from the condition of minimum energy. The calculations showed that the purely ionic states correspond to 12% of the total energy of the bond. The energy of the bond itself is 0.21 at units.

Conclusions: According to Pauling's empirical formula the ionic component of the binding in the SiC crystal is also 12%. It should be noted, however, that Pauling's formula gives this fraction of energy only for the ionic state where both electrons are on the more electronegative atom, i.e., on the C atom in our case. The corresponding fraction of energy is 9% according to our calculations. Furthermore, Pauling's formula does not account at all for the role of mixed states.

Finally, we must note that more precise results could be obtained by using for wave functions the ψ functions proposed elsewhere, which are very close to the Hartree functions. However, we did not use these functions because they complicate the calculations while increasing the precision relatively little.

Photoconductivity Theory Based on Variations of Carriers Mobility, Sh. M. Kogan, pp. 1386-1389

When variations of the carrier energy spectrum due to irradiation can be represented by changes in the electron temperature, photoconductivity based on variation of carrier mobility is determined by the nonlinearity of the direct current voltage characteristic. The expression obtained for the photoresponse, in particular, takes into account the variation in the power supplied by the battery during absorption of the irradiation. The electronic thermal conductivity has no effect on the photoresponse.

Photomagnetic emf in *p*-Type InSb at Room Temperature in an Alternating Magnetic Field, V. F. Zolotarev and D. N. Nasledov, pp. 1428-1431

We have investigated the photomagnetic emf in *p*-type InSb in an alternating magnetic field with a constant light intensity. The photomagnetic emf is twice as large as in a steady magnetic field. In an alternating magnetic field the photomagnetic emf in InSb consists of a sum of odd harmonics. The proposed method of investigating photo-, thermo-, and galvanomagnetic phenomena with an alternating magnetic field makes it possible to find several more experimental dependences from one experiment than are possible with a steady magnetic field.

Volume 4, Number 8, February 1963

High-Voltage Photo-emf's in Layers of Antimony Triselenide, V. M. Lyubin and G. A. Fedorova, pp. 1486-1489

The results of a study of electrical and photoelectric properties are reported for sublimated crystalline layers of antimony triselenide, in which photo emf's up to 50-80 v/cm were generated on illumination. In addition parameters are given for layers of some chalcogenides of antimony and bismuth in which high-voltage photo emf's were also observed.

It has recently been shown that high voltage photo emf's, up to 100 v/cm, can be generated in layers of cadmium telluride prepared by evaporation in vacuum with oblique incidence of the molecular beam. Goldstein and Pensak proposed a model in which the appearance of high photo emf's can be accounted for by summation of emf's produced by illumination of individual "photovoltaic elements" in the layer. "Ordering" is then due to the oblique incidence of the molecular beam.

In an earlier paper we described experiments showing that the model of Goldstein and Pensak is unsatisfactory and that the generation of high photo emf's in CdTe layers is a complex phenomenon. In the same paper we reported the preparation and

high photo emf's of layers of some chalcogenides of antimony and bismuth. The present paper gives the results of a study of antimony triselenide layers in which photo emf's up to 50-80 v/cm were generated.

Strengthening of Glass, F. F. Vitman, I. A. Boguslavskii, and V. P. Pukh, pp. 1582-1587

We propose a two-stage method for strengthening glass: first, quenching in liquids, and then etching in hydrofluoric acid. We show that this method makes it possible to reach unheard-of strength—100 kg/mm²—for glass 1.5 to 5 mm thick (as compared to an original strength of 10 kg/mm²). We discuss the reasons that quenching induces high strength. We show that this strengthening, occurring at both high and relatively low cooling rates, is due not only to surface compression stresses but also to physical changes in the surface layers.

Conclusions: We have shown earlier that the well known method of strengthening glass by etching in HF solutions insures additional strength in glass previously quenched in air. In the present investigation this two stage method (quenching + etching) was applied to glasses quenched in liquids. The results in this investigation, together with the results of a special study of quenching stresses in glass, allow us to draw the following conclusions:

1) Quenching glass 1.5-3 mm thick in air does not result in any noticeable strengthening. This means that quenching in air is much less important for thin glass than for thick glass, whose strength can be increased to 70-75 kg/mm² by quenching and etching.

2) The strength of thin glass (up to 5-6 mm thick) can be increased to 100 kg/mm² by quenching in warm silicone or mineral oils followed by etching in HF solutions. The cooling rate of glass during quenching differs according to the liquid used, and the increase in the average strength of glass as the result of quenching is from 10-20 to 30-80 kg/mm². Etching gives an additional increase in the average strength of these glasses to 60-125 kg/mm².

3) The minimum strength of glass 1.5-3 mm thick treated in this manner becomes at least 50 kg/mm², a value never reached before.

4) The strengthening of glass resulting from quenching either in air or in liquids cannot be explained by the creation of surface compression stresses alone. A considerable part of the increase in strength resulting from quenching must be due to physical changes in the surface layer of the glass; the higher the cooling rate during quenching, the greater this part is.

5) The two stage method investigated here, consisting in quenching glass in liquids and etching in solutions of HF, makes it possible to obtain very high strength, and should be developed on an industrial scale and applied to large pieces of glass, which would solve a number of technological problems.

The First Diffusion Equation, R. L. Fogel'son, pp. 1661-1662

Usually the first equation of diffusion is derived by considering diffusion as simple transport of particles due to a concentration gradient. Then, if it is assumed that the probability of displacement of an atom from one equilibrium position to a neighboring one is independent of the direction of this displacement, the first equation of diffusion is obtained in its usual form

$$j = -D(\partial n / \partial x) \quad (1)$$

Since this equation does not exactly represent the experimental situation in heterodiffusion, it is natural to assume that the probabilities of displacements in the forward and backward directions are different. Then, the first equation of diffusion becomes

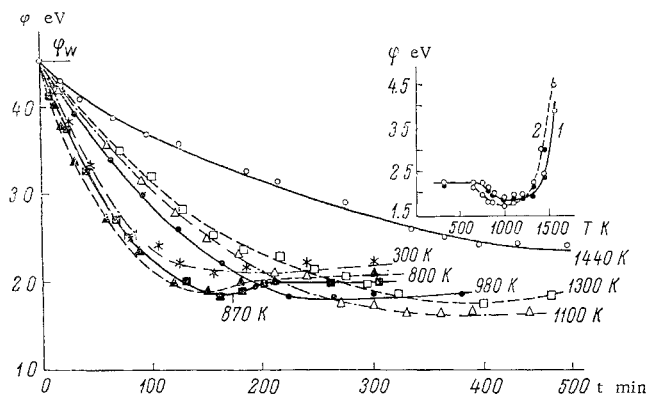
$$j = -(\partial / \partial x)(D^*n) \quad (2)$$

We shall show that even this equation is not confirmed by experiment. Consequently a derivation of the diffusion equation on the assumption of simple transport of matter is not quite correct for actual processes, because some of the factors important in these processes are not taken into account. If there is a concentration gradient the probabilities of displacements of atoms in opposite directions should differ at any given point, but the probabilities for that point should have something in common which differentiates them from the displacement probabilities at other points. It is possible that a derivation similar to that used for the viscous flow of liquids represents actual processes more correctly.

Volume 4, Number 9, March 1963

Data Relating to the Production of Lead Sulfide Single Crystals, I S Aver'yanov, N S Baryshev V G Baru, and G I Yudina, pp 1720-1724

Lead sulfide single crystals of n - and p type with carrier concentrations up to 10^{17} cm^{-3} were grown by the Bridgman Stockbarber method. We have investigated the process of PbS crystal growth from the melt with due regard to interaction between the solid and vapor phases. The reasons underlying the creation of p n junctions during the growth of lead sulfide single crystals are discussed. We have examined the possibility of controlling the characteristics of PbS single crystals by treatment and zone melting in sulfur vapor. We have evaluated numerically the accuracy to which the operating conditions must be stabilized at various annealing temperatures in order to obtain specimens with carrier concentrations of the order of $5 \times 10^{16} \text{ cm}^{-3}$. We have obtained a general formula for the equilibrium sulfur pressure which takes into account the existence of donor and acceptor impurities.

Work Function of Thin Layers of Barium Oxide Deposited on Hot Tungsten, T S Kirsanova, A R Shul'man, and A V Dement'eva, pp 1918-1919

Dependence of the work function of the BaO - W system on the duration of deposition for various substrate temperatures. In the inset curve 1 shows dependence of equilibrium work function on substrate temperature, and curve 2 gives dependence of quasi-equilibrium work function on temperature of subsequent treatment. Different rates of deposition are denoted by different point

It has been shown that the heating of barium oxide layers deposited onto cold tungsten and molybdenum foils at comparatively low temperatures (1000-1200 K) increases the thermionic activity: The work function of the BaO-W system is reduced, compared with its value immediately after deposition. The present paper describes the results of experiments on changes in the work function of BaO-W systems prepared by deposition of barium oxide onto tungsten foil kept at various temperatures.

Changes in the Surface Potential of Lead Sulfide Layers on Illumination, R Ya Berlaga and T T Bykova, pp 1929-1930

Changes in the surface potential of polycrystalline layers of lead sulfide on illumination were determined by measuring the changes in the contact potential difference between PbS and a standard electrode using modulated illumination.

SOVIET PHYSICS—DOKLADY (Doklady Akademii Nauk SSSR, Otdelenie Fiziki) Published by American Institute of Physics, New York

Volume 7, Number 1, July 1962

Determination of the Physical Properties of the Cyanogen Envelopes of Halley's Comet, 1910—II, D O Moknach, pp 1-3**Splitting of Nonevolutionary Magnetohydrodynamic Shock Waves, V V Gogosov, pp 10-12**

In this paper a method is proposed allowing one to determine into which combination of evolutionary discontinuities and pro-

gressing expansion waves a magnetohydrodynamic shock wave will split (decompose). No assumptions are imposed on the parameters of the medium or intensity of the shock.

Evolution discontinuities are discontinuous solutions of nonlinear differential equations which depend continuously on the initial and boundary conditions. Thus, gasdynamic or magnetohydrodynamic shock waves will be evolutionary if small changes in the gasdynamic or magnetohydrodynamic quantities result in small changes in the solution. The first idea of evolutionarity was expressed in references noted in connection with the study of discontinuities in ordinary gas dynamics.

General Theory of Steady Motion in Relativistic Hydrodynamics, I S Shikin, pp 13-14

We shall investigate the steady adiabatic motion of an ideal gas in relativistic hydrodynamics (within the framework of the special theory of relativity). We shall consider the entropy in general to differ from one streamline to another. In this paper, it is shown that each such motion reduces to the nonrelativistic motion of some gas. The potential plane parallel motion of an ultrarelativistic gas was shown in another paper.

Interpretation of Nonstationary Relativistic Hydrodynamics in Minkowski Space, I S Shikin, pp 15-17

We will consider the adiabatic motion of a perfect nonviscous gas in relativistic hydrodynamics (without taking gravitational fields into account). As was shown elsewhere, every steady motion in relativistic hydrodynamics can be treated as nonrelativistic, steady motion of a corresponding gas. It is shown here that nonsteady motion in relativistic hydrodynamics can be treated, in the same quantities in four dimensional space time, as nonrelativistic steady motion, assuming that the constant in the Bernoulli equation is 0.

Structure of Relativistic Nonlinear Waves in a Plasma, V N Tsytoich, pp 31-33

When a relativistic beam of charged particles passes through a plasma, waves which are propagated with a speed close to that of light are excited in the plasma. The linear approximation for the treatment of waves in the system can serve only to estimate the time of development of the nonlinear motion in terms of the logarithmic increment of the oscillations. Nonrelativistic nonlinear waves in a plasma have been considered in other papers. Here we wish to call attention to a number of interesting properties of relativistic nonlinear waves, and also to use the example of two mutually penetrating identical plasmas to illustrate the solution of a nonlinear problem of the energy loss of a beam in a plasma.

In writing the system of equations with which we begin we shall assume that: 1) the use of the hydrodynamical approximation of zero temperatures to describe the plasma and the beam; 2) the ions which initially compensate the space charges of the plasma and the beam are stationary; 3) the motion is one dimensional (depends on the time x_0 and the coordinate x).

Impact Compressibility of Liquid Nitrogen and Solid Carbon Dioxide, V N Zubarev and G S Telegin, pp 34-36

The experimental investigations of the compressibility of N_2 and CO_2 by static methods relate to the region of comparatively low pressures and densities. Thus, for N_2 the greatest pressure ($P = 15,000 \text{ atm}$) and densities ($\rho = 1.1 \text{ g/cm}^3$) were achieved by Bridgman in the isothermal compression of nitrogen ($T = 338 \text{ K}$). More detailed investigations of the equations of state for these substances were conducted at still lower pressures. The aim of the present work was to reach pressures of hundreds of thousands of atmospheres and densities of $\sim 2-3 \text{ g/cm}^3$ in substances which form the bulk of explosion products obtained in the detonation of condensed explosives.

Volume 7, Number 2, August 1962

Theory of Gyroscope Follow-Up in the Presence of Random Interference, L Ya Roitenberg, pp 110-113

A gyroscope follow-up is a gyro with three degrees of freedom operating in accordance with the gyroscope stabilization principle. The axis of the outside Cardan ring of the gyro is vertical and the axis of its case horizontal. The outside Cardan ring should follow the useful input signal transmitted from without, from some actuating system. The input signal consists of a useful signal plus interference, the latter being represented by a stationary random process whose correlation function is assumed to be known. In the present article the optimum reproduction of the